Simulation of high-frequency capacitance-voltage characteristics of amorphous/crystalline heterojunctions

Hideharu M. Matsuura
Electrotechnical Laboratory, 1-1-4 Umezono, Tsukuba, Ibaraki 305, Japan

(Received 27 December 1989; accepted for publication 27 March 1990)

The model for simulating high-frequency capacitance-voltage characteristics of amorphous/crystalline heterojunctions has been developed, where the high frequency indicates a frequency higher than the reciprocal of the dielectric relaxation time of the amorphous semiconductor. The physical background of the space-charge density of the amorphous film and the built-in voltage of the heterojunction, which are experimentally obtained from the heterojunction-monitored capacitance method, is discussed using the calculated results.

I. INTRODUCTION

Measurements of capacitance-voltage (C-V) characteristics of junctions are very important for determining space-charge densities of crystalline semiconductors because the theory of the C-V characteristics has already been established.[1] In the case of amorphous semiconductors, however, the theory of the C-V characteristics has not been well developed, although many researchers have theoretically investigated C-V characteristics of Schottky barrier junctions[2-17] as well as those of amorphous/crystalline heterojunctions.[18-21] There are two main problems when one simulates the C-V characteristics: One is how to deal with energetically distributed localized states in the gap, and the other is how to treat the frequency dependence of capacitance, which is related to the dielectric relaxation time of the amorphous film and the trapping/detrapping time of carriers at the localized states. Because of the latter problem, most models can accurately simulate only zero-frequency C-V characteristics which cannot experimentally be measured. For instance, although a plot of the inverse square of the capacitance of Schottky barrier junctions measured at a low frequency yields a straight line,[22,23] the physical background of the apparent space-charge density and the apparent built-in voltage obtained from the plot is not yet clear.

We have recently developed the heterojunction-monitored capacitance (HMC) method[24-28] which can experimentally determine midgap-state densities in undoped hydrogenated amorphous semiconductors from high-frequency (1 MHz) C-V characteristics of amorphous/crystalline heterojunctions. Since this frequency is high enough to be able to neglect the dielectric relaxation process as well as the trapping/detrapping process in the amorphous film, one only requires the thickness of the amorphous film and the width of the depletion region in the crystalline semiconductor produced by dc reverse bias in order to calculate the capacitance, indicating that it is able to simulate accurately the high-frequency C-V characteristics of amorphous/crystalline heterojunctions. In this paper, we simulate the high-frequency C-V characteristics. The model for simulating the C-V characteristics adopts (1) one kind of density-of-state distribution $g(E)$ in the amorphous semiconductor, instead of two kinds of $g(E)$'s, i.e., donorlike and acceptorlike $g(E)$'s, and (2) the carrier occupation function of the localized states in the depletion region, which is derived from emission rates for electrons and holes, instead of the Fermi–Dirac distribution function, because we consider amorphous/crystalline heterojunctions which exhibit rectifying properties in current-voltage (I-V) characteristics to be different from metal-oxide-semiconductor (MOS) diodes. Those assumptions were already used for Schottky barrier junctions.[12,13] Furthermore, we discuss the validity of the HMC method.

II. MODELING

Let us consider an undoped (slightly n-type) amorphous/p-type crystalline silicon (n-a-Si:H/p-c-Si) heterojunction. Figure 1 shows an energy-band diagram, a potential $u(x)$ for electrons, space charges produced by dc reverse bias (V_{dc}), and charges (dQ_{ac}) in response to a small high-frequency ac voltage to measure the capacitance. The differences between the depletion region ($0 \leqslant x \leqslant W_2$) and the neutral region ($x > W_2$) are (1) whether localized states below the Fermi level (E_F) trap electrons or not, and (2) whether electrons exist in the conduction band as well as in the conduction-band tail or not. These changes result in the space charge in the depletion region of a-Si:H. In this analysis, therefore, the density of charged states in both neutral and depletion regions is not necessary to be taken into consideration.

In the neutral region, for example, the electron concentration (n) in the conduction band of undoped a-Si:H is about 6×10^{9} cm^{-3}, which is calculated using the relation $\sigma_2 = q\mu_2 n$, where the dark conductivity (σ_2) is 10^{-9} S/cm, the electron charge (q) is 1.6×10^{-19} C, and the drift mobility (μ_2) is 1 cm^2/V/s. Since this value is much smaller than the space-charge density ($\geqslant10^{15}$ cm^{-3}, which is the experimentally obtained value) in the depletion region of undoped a-Si:H, the contribution of the electrons in the conduction band to the production of the space charge can be neglected. The electron density (n_{BT}) in the conduction-band tail at room temperature can be estimated as

$$n_{BT} = \int_{E_F^a}^{E_C} f(E)N(E_C)\exp[-(E_C - E)/E_{BT}]\,dE, \tag{1}$$

 0021-8979/90/151138-05$03.00

where $f(E)$ is the Fermi–Dirac distribution function, $N(E_C)$ is the density at the bottom of the conduction band, E_F^a is the Fermi level in the neutral region of a-Si:H, and E_{BT} is the characteristic energy for the conduction-band tail. The value of n_{BT} is 2×10^{13} cm^{-3} using $N(E_C)=10^{21}$ cm^{-3} eV^{-1}, $(E_C-E_F^a)=0.73$ eV, and $E_{BT}=50$ meV, suggesting that the contribution of the electrons in the conduction-band tail to the production of the space charge can also be neglected. Since E_{BT} of 50 meV is overestimated,[29] other localized states above E_F^a must be hidden by the assumed conduction-band tail states. Therefore, localized states below the Fermi level mainly produce the positive space charge in the depletion region. The space-charge density (ρ) at the spatial position (x) is expressed as

$$\rho[u(x)]=q\int_{E_F^a-u(x)}^{E_F^a} g(E)dE, \tag{2}$$

where $g(E)$ is the density-of-state distribution in a-Si:H. Here, for the sake of simplicity, the Fermi–Dirac distribution function and the occupation function for electrons at the localized states are approximated by step functions.

The carrier densities in the conduction and valence bands in the depletion region are governed by the quasi-Fermi levels.[10,30] The quasi-Fermi level (E_{Fn}) for electrons is almost constant in the depletion region and rises toward the Fermi level near the edge of the depletion region of p-c-Si, while the quasi-Fermi level (E_{Fp}) for holes falls near the edge of the depletion region of a-Si:H, as shown in Fig. 1(a).

In region II ($0\leqslant x\leqslant W_{OB}$) where E_{Fn} is below E_{OB}, the space-charge density is kept constant, and it is expressed as

$$\rho(u_{OB})=q\int_{E_{OB}^a}^{E_F^a} g(E)dE, \tag{3}$$

and

$$qN_D\equiv\rho(u_{OB}), \tag{4}$$

with

$$u_{OB}\equiv E_F^a-E_{OB}^a, \tag{5}$$

where N_D is the real midgap-state density between E_F^a and E_{OB}^a in the a-Si:H, E_{OB}^a is E_{OB} in the neutral region of a-Si:H, and E_{OB} is determined from the condition that the thermal-emission rate for electrons is equal to that for holes, given by[27,30]

$$E_{OB}=E_m+(kT/2)\ln(\nu_p/\nu_n), \tag{6}$$

because the I-V characteristics of the heterojunction are quite similar to those of p-n junctions,[24,25] not to those of MOS diodes. Here, E_m is the midgap $(E_C-E_V)/2$, and ν_p and ν_n are the attempt-to-escape frequencies for holes and electrons, respectively. This concept is important for discussing the occupation of the deep levels in the depletion region of the diode which exhibits a rectifying property in I-V characteristics.[12,13,27,30] This concept produces the constant space-charge density in the part of the depletion region of a-Si:H, and it is different from the concept used by Rubinelli *et al.*[18-20] and Xu *et al.*[21] In their simulations of zero-frequency C-V characteristics, two kinds of localized states (i.e., donorlike and acceptorlike states) are considered. Donorlike states above E_{Fp} are positively charged, and acceptorlike states below E_{Fn} are negatively charged. As is clear from Fig. 1(a), since the densities of positively and negatively charged states depend on the spatial position, the net space-charge density is not constant even in region II.

At thermal equilibrium (i.e., $V_{dc}=0$ V), when the built-in potential for a-Si:H is larger than the value of $(E_F^a-E_{OB}^a)$, $\rho(x)$ near the interface exceeds qN_D because the Fermi level is below E_{OB} near the interface. This situation near the interface is held even when the reverse bias is applied. However, the contribution of the excess charges near the interface should be taken into account as the effect of charged states in the near-interface region which is mentioned later.

On the other hand, in region I ($W_{OB}<x\leqslant W_2$), where E_{Fn} is above E_{OB}, Eq. (2) is valid. In the depletion region in p-c-Si (region III, $-W_1\leqslant x<0$), according to the depletion approximation, the space-charge density is given by $-qN_A$, where N_A is the acceptor density of p-c-Si since p-c-Si has only shallow acceptors. As a consequence, the space-charge density can be schematically shown in Fig. 1(c). The following items are required from the approximations [Eqs. (2) and (6)]: (1) Space-charge density in the depletion region of the amorphous film is much larger than the carrier densities in the conduction and valence bands in the neutral region of the amorphous film, which is satisfied by highly resistive a-Si:H films, and (2) heterojunctions should exhibit a rectifying property in I-V characteristics, which is satisfied by undoped a-Si:H/p-c-Si heterojunctions.

III. ESTIMATION

The potential $u(x)$ for electrons can be determined from Poisson's equation

$$d^2[u(x)/q]/d^2x=\rho/\epsilon_s, \tag{7}$$

where ϵ_s is the semiconductor permittivity. For shortness' sake, ϵ_{s1} for c-Si is assumed to equal ϵ_{s2} for a-Si:H. The space charge Q_I in region I ($W_{OB}<x\leqslant W_2$) is given by[1]

$$Q_I=\left(2\epsilon_s\int_0^{u_{OB}}\rho(u)du\right)^{1/2}, \tag{8}$$

and the electric field (E_I) at $x=W_{OB}$ is given by[1]

$$E_I=Q_I/\epsilon_s. \tag{9}$$

In region II, Eq. (7) can easily be solved with the boundary conditions that $u(0)\equiv u_0$, $du/dx=E_I$ at $x=W_{OB}$, and $u(W_{OB})\equiv u_{OB}$, because $\rho=qN_D$, where N_D is constant in the region. The value of W_{OB} is calculated as a function of u_0. Then, the width (W_1) of the depletion region in p-c-Si is estimated from the charge neutrality

$$qN_AW_1=qN_DW_{OB}+Q_I, \tag{10}$$

and the reverse voltage (V_{dc}) is calculated from the relation

$$V_D-V_{dc}=u_0/q+qN_AW_1^2/2\epsilon_s, \tag{11}$$

where V_D is the built-in voltage. Finally, the high-frequency capacitance (C) is estimated as

$$C=\epsilon_sS/(W_1+L), \tag{12}$$

because, spatially, the redistribution of charged carriers can

respond to the high-frequency ac voltage at W_1 and L due to the long dielectric relaxation time (ϵ_{s2}/σ_2) of undoped *a*-Si:H, as shown in Fig. 1(d). Here, L is the thickness of *a*-Si:H, σ_2 is the dark conductivity of the amorphous film, and S is the electrode area. As for the localized states in the amorphous film, we tentatively assume a Gaussian distribution of localized states:

$$g(E) = g_{\max} \exp[-(E - E_p)^2/2E_W^2], \tag{13}$$

because main localized states in the midgap are assigned to be dangling bonds.

Let us consider interface states as well as states of the near-interface region which is a qualitatively different layer (about 50 Å) near the interface from the bulk.[31] In this paper, we assume one kind of positively charged layer with the thickness of d_s and the density of N_s between *p-c*-Si and *a*-Si:H in place of the interface and the near-interface region. This representative layer is called an interface layer in this paper, and the charge Q_{ss} per unit area is given by $N_s d_s$.

Since we would like to know the physical background of the space-charge density as well as the built-in voltage obtained from the HMC method which is described in the next section, almost all of parameters for the simulation are fixed, as shown in Table I.

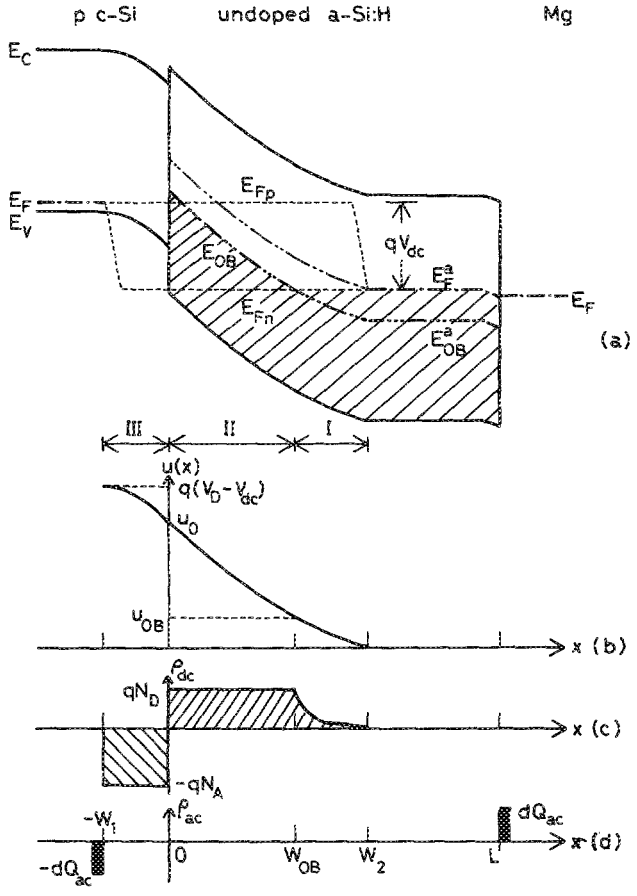

FIG. 1. Schematic sketches of the heterojunction: (a) energy-band diagram, (b) potential variation for electrons, (c) space-charge density for dc reverse bias, and (d) charge in response to a small high-frequency ac voltage to measure capacitance. The localized states as indicated by the hatched area of (a) are full of electrons. Magnesium (Mg) is used to get an ohmic contact with undoped *a*-Si:H.

IV. HETEROJUNCTION-MONITORED CAPACITANCE METHOD

Let us consider the HMC method[23-28] which can experimentally determine the midgap-state densities (N_I) in amorphous semiconductors as well as the built-in voltages (V_B) of these heterojunctions from high-frequency *C-V* characteristics. In the HMC method, we neglected region I shown in Fig. 1 as well as the interface layer. We adopted the depletion approximation in both depletion regions. We can easily derive the relation

$$W_I^2 = [\epsilon_s(1/C - 1/C_2)]^2 \tag{14}$$

$$= 2\epsilon_s N_I (V_B - V_{dc})/qN_A(N_A + N_I), \tag{15}$$

where C is the capacitance measured at a frequency higher than $\sigma_2/2\pi\epsilon_s$ of the amorphous film, C_2 is the saturated capacitance at higher forward bias which is equal to the geometric capacitance of the *a*-Si:H, N_I is the density of the midgap states which should correspond to N_D in Sec. III, and V_B is the built-in voltage which should correspond to V_D in Sec. III. The $W_I^2 - V_{dc}$ relation is obtained from the *C-V* characteristics using Eq. (14), and then N_I and V_B can be graphically estimated using Eq. (15). In the following section, we compare N_I and V_B obtained from the HMC method with the parameters (N_D and V_D) for the simulation.

V. RESULTS AND DISCUSSIONS

A. *C-V* characteristics without the interface layer

Figure 2(a) shows the calculated high-frequency *C-V* characteristics of an amorphous/crystalline heterojunction with parameters of $g_{\max} = 10^{16}$ cm^{-3} eV^{-1} and $N_A = 10^{15}$ cm^{-3}, and Fig. 2(b) shows the W_I^2-V_{dc} relation replotted from the data of the *C-V* characteristics in Fig. 2(a) using Eq. (14). According to Eq. (15), N_I and V_B can be graphically obtained from the slope and the intercept on the abscissa, respectively. The value of N_I obtained in the reverse range $-6\text{ V} \leqslant V_{dc} \leqslant -1\text{ V}$ is 2.5×10^{15} cm^{-3}, and it is close to N_D of 2.0×10^{15} cm^{-3}, where N_D is calculated from Eqs. (3) and (4) using the given parameter of $g_{\max} = 1\times10^{16}$ cm^{-3} eV^{-1}. The value of V_B, which is obtained from the intercept of the straight line drawn in the reverse-bias range $-6\text{ V} \leqslant V_{dc} \leqslant -1\text{ V}$ on the abscissa, is 0.21 V, and it is a little lower than the given parameter of $V_D = 0.30$ V because the additional potential u_{OB} is necessary to make the space-charge density constant.

Figure 3 depicts N_I and V_B as a function of N_D. Figure 4 shows the dependence of N_I and V_B on N_A. From both figures, N_I represents the midgap-state density well, although N_I is a little larger than N_D.

B. *C-V* characteristics with the interface layer

The calculated high-frequency *C-V* characteristics with the interface layer are similar to Fig. 2, although the lowest reverse bias, where the discrepancy from the straight line starts to occur, is higher than the reverse bias (about 0.7 V)

TABLE I. Parameters used for simulating high-frequency C-V characteristics.[a,b]

Amorphous film			
Neutral region	Midgap states	Interface layer	Others
$E_C - E_F^a = 0.73$ eV	$E_C - E_p = 0.85$ eV	$N_s = 0$–10^{18} cm^{-3}	$V_D = 0.3$ V
$E_C - E_{OB}^a = 0.97$ eV	$E_W = 0.10$ eV	$d_s = 0$ or 50 Å	$L = 1.2\ \mu$m
	$g_{max} = 10^{16}$–10^{17} cm^{-3} eV^{-1}		$S = 0.785$ mm^2
			$N_A = 10^{15}$–10^{17} cm^{-3}

[a] N_D is calculated from Eq. (4) using the given g_{max}.
[b] N_I and V_B obtained from the HMC method correspond to the parameters N_D and V_D for the simulation, respectively.

calculated without the effect of the interface layer. Figure 5 shows the dependence of N_I and V_B on the charge ($Q_{ss} = N_s d_s$) with $g_{max} = 3\times10^{16}$ cm^{-3} eV^{-1} and $N_A = 10^{16}$ cm^{-3}. In the range $N_s \leqslant 2\times10^{17}$ cm^{-3} or $Q_{ss} \leqslant 10^{11}$ cm^{-2}, the values of N_I and V_B are quite close to given N_D and V_D, respectively, and then they rapidly increase with N_s. These increases result from Q_{ss}.

C. Validity of the HMC method

As is clear from the results with low Q_{ss}, N_I and V_B obtained from the HMC method represent the real midgap-state density and the real built-in voltage quite well, respectively. The value of Q_{ss} is important for discussing the validity of the HMC method, but the experimental determination of Q_{ss} is quite difficult.

On the other hand, it is easy to determine experimentally whether N_I is close to the real midgap-state density. It is judged from the value of V_B, as is clear from Fig. 5. For example, since V_B obtained from the HMC method is close to V_B roughly obtained from current-voltage characteristics,[24,25] N_I must be close to the real midgap-state density. In fact, N_I experimentally obtained was close to the bulk spin density obtained from electron-spin-resonance measurements where surface-state contributions were estimated by results from a series of films over a range of thickness,[32] indicating that N_I represents the density of singly occupied dangling bonds (i.e., the midgap-state density). Moreover, V_B experimentally obtained is reasonable for explaining the properties of amorphous/crystalline silicon heterojunction bipolar transistors.[25,33] From the above experimental results, Q_{ss} must be small enough to neglect the effect of the

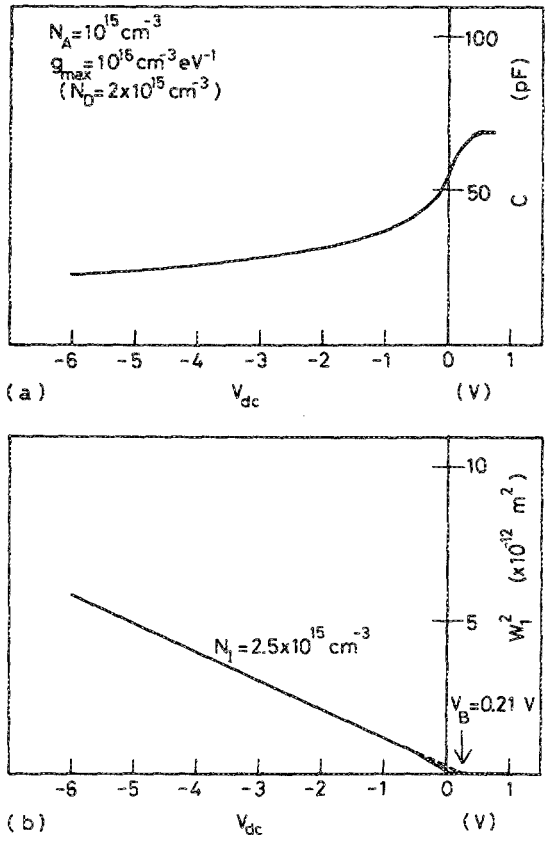

FIG. 2. Calculated results without the interface layer: (a) capacitance-voltage characteristics and (b) the voltage dependence of the square of the depletion width in the crystalline semiconductor. The values of N_I and V_B are obtained from the HMC method. The solid line is the calculated data, and the dashed line is the line extrapolated from higher reverse bias.

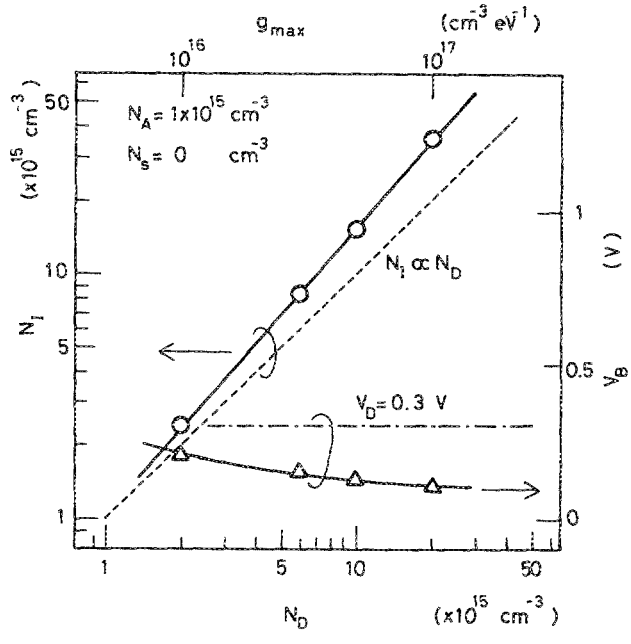

FIG. 3. The dependencies of N_I and V_B obtained from the HMC method on the real donorlike state density N_D without the interface layer. The values of N_I and V_B correspond to parameters (N_D and V_D) for simulating the high-frequency C-V characteristics, respectively.

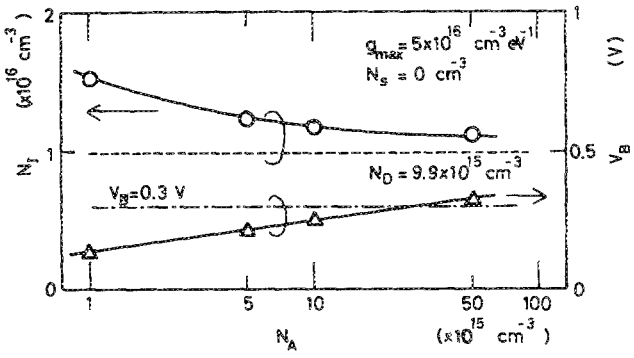

FIG. 4. The dependencies of N_I and V_B obtained from the HMC method on the acceptor density in the crystalline semiconductor without the interface layer.

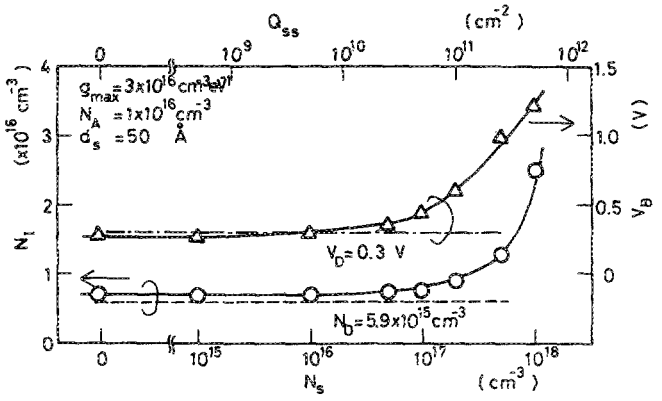

FIG. 5. The dependencies of N_I and V_B obtained from the HMC method on the density of the interface layer.

interface states in the case of undoped a-Si:H deposited by normal rf glow discharge.

VI. CONCLUSION

In order to discuss the validity of the HMC method which we developed earlier, the high-frequency C-V characteristics of amorphous/crystalline heterojunctions have been simulated. Trapping and detrapping processes of carriers at localized states as well as carrier redistribution in the extended states in amorphous semiconductors cannot respond to the ac voltage because the measuring frequency is much higher than the reciprocal of the dielectric relaxation time of the amorphous film, indicating that the thickness of the amorphous film as well as the width of the depletion region in the crystalline semiconductor produced by dc reverse bias are only required to calculate the high-frequency capacitance. Therefore, the simulation of the C-V characteristics has been found to be accurate and easy. In the reasonable case that Q_{ss} is less than 10^{11} cm^{-2}, N_I and V_B obtained from the HMC method represent the midgap-state density of the amorphous film and the built-in voltage of the heterojunction, respectively.

ACKNOWLEDGMENT

The author wishes to acknowledge his gratitude to the members of the staff of the Non-Equilibrium Materials Section in the Electrotechnical Laboratory for their valuable insights and comments.

[1] S. M. Sze, *Physics of Semiconductor Devices*, 2nd ed. (Wiley-Interscience, New York, 1981).
[2] W. E. Spear, P. G. LeComber, and A. J. Snell, Philos. Mag. B **38**, 303 (1978).
[3] A. J. Snell, K. D. Mackenzie, P. G. LeComber, and W. E. Spear, Philos. Mag. B **40**, 1 (1979).
[4] J. Singh and M. H. Cohen, J. Appl. Phys. **51**, 413 (1980).
[5] P. Viktorovitch and G. Moddel, J. Appl. Phys. **51**, 4847 (1980).
[6] P. Viktorovitch and D. Jousse, J. Non-Cryst. Solids **35&36**, 569 (1980).
[7] J. Beichler, W. Fuhs, H. Mell, and H. M. Welsch, J. Non-Cryst. Solids **35&36**, 587 (1980).
[8] T. Tiedje, C. R. Wronski, and J. M. Cebulka, J. Non-Cryst. Solids **35&36**, 743 (1980).
[9] P. Viktorovitch, J. Appl. Phys. **52**, 1392 (1981).
[10] C. H. Hyun, M. S. Shur, and A. Madan, J. Non-Cryst. Solids **46**, 221 (1981).
[11] R. A. Abram and P. J. Doherty, Philos. Mag. B **45**, 167 (1982).
[12] J. D. Cohen and D. V. Lang, Phys. Rev. B **25**, 5321 (1982).
[13] T. Suzuki, Y. Osaka, and M. Hirose, Jpn. J. Appl. Phys. **22**, 785 (1983).
[14] D. Jousse and S. Deleonibus, J. Appl. Phys. **54**, 4001 (1983).
[15] A. Glade, W. Fuhs, and H. Mell, J. Non-Cryst. Solids **59&60**, 269 (1983).
[16] H. L. Fernandez-Canque, J. Allison, and M. J. Thompson, J. Appl. Phys. **54**, 7025 (1983).
[17] I. W. Archibald and R. A. Abram, Philos. Mag. B **54**, 421 (1986).
[18] F. Rubinelli, S. Albornoz, and R. Buitrago, Solid-State Electron. **28**, 741 (1985).
[19] F. A. Rubinelli, M. R. Battioni, and R. H. Buitrago, J. Appl. Phys. **61**, 650 (1987).
[20] F. A. Rubinelli, Solid-State Electron. **30**, 593 (1987).
[21] Z. Y. Xu, W. Chen, B. F. Zhao, C. A. Wang, F. Q. Zhang, and J. Y. Wang, J. Non-Cryst. Solids **97&98**, 983 (1987).
[22] C. R. Wronski and D. E. Carlson, Solid State Commun. **23**, 421 (1977).
[23] H. Matsuura and H. Okushi, J. Appl. Phys. **62**, 2871 (1987).
[24] H. Matsuura, T. Okuno, H. Okushi, and K. Tanaka, J. Appl. Phys. **55**, 1012 (1984).
[25] H. Matsuura, IEEE Trans. Electron Devices **ED-36**, 2908 (1989).
[26] H. Matsuura, Jpn. J. Appl. Phys. **27**, L513 (1988).
[27] H. Matsuura, J. Appl. Phys. **64**, 1964 (1988).
[28] H. Matsuura and K. Tanaka, Mater. Res. Soc. Symp. Proc., Vol. 118, edited by A. Madan, M. J. Thompson, P. C. Taylor, P. G. LeComber, and Y. Hamakawa (Materials Research Society, Pittsburgh, 1988), p. 647.
[29] S. Yamasaki, H. Oheda, A. Matsuda, H. Okushi, and K. Tanaka, Jpn. J. Appl. Phys. **21**, L539 (1982).
[30] E. H. Rhoderick and R. H. Williams, *Metal-Semiconductor Contacts*, 2nd ed. (Clarendon, Oxford, 1988), p. 162.
[31] R. W. Collins and J. M. Cavese, J. Non-Cryst. Solids **97&98**, 269 (1987).
[32] H. Matsuura, Z E. Smith, A. Matsuda, S. Yokoyama, M. Tanaka, M. Ueda, and K. Tanaka, Philos. Mag. Lett. **59**, 109 (1989).
[33] J. Symons, M. Ghannam, J. Nijs, A. van Ammel, P. de Schepper, A. Neugroschel, and R. Mertens, Appl. Phys. A **41**, 291 (1986).